Chapter 7: Robustness in bacterial chemotaxis 30/4/18-TSB

7.1 Introduction

We saw how bifunctional proteins can make the input-output relation of a signaling circuit precise despite variation in protein levels. But not all signaling circuits need to simply transduce the signal level. Some circuits are built to make more sophisticated computations, and to do so robustly. To see this, we will now consider the robustness of a remarkable protein circuit called the **bacterial chemotaxis** circuit, that allows bacteria to navigate. Bacterial chemotaxis is so well-characterized on the level of both molecules and behavior that it is a testing ground for important ideas in systems biology, including robustness. We will describe the biology of bacterial chemotaxis, and models and experiments that demonstrate how the computation performed by this protein circuit is made robust to changes in protein levels. We will see that the principle of robustness can help us to rule out many plausible mechanisms and to home in on the correct design.

7.2 Bacterial chemotaxis, or how bacteria think

7.2.1 Chemotaxis behavior

When a pipette containing nutrients is placed in a plate of swimming *Escherichia coli* bacteria, the bacteria are attracted to the mouth of the pipette and form a cloud (Figure 7.1). When a pipette with noxious chemicals is placed in the dish, the bacteria swim away from the pipette. This process, in which bacteria sense and move along gradients of specific chemicals, is called **bacterial chemotaxis**.

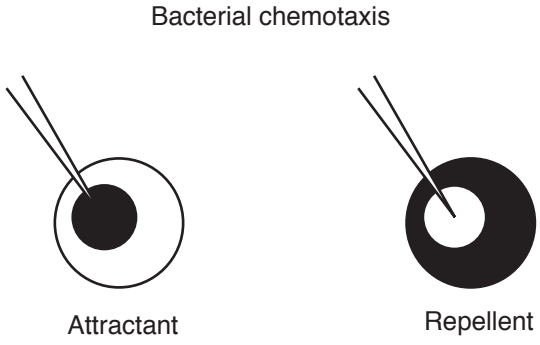

Figure 7.1

Chemicals that attract bacteria are called **attractants**. Chemicals that drive the bacteria away are called **repellents**. *E. coli* can sense a variety of attractants, such as sugars and the amino acids serine and aspartate, and repellents, such as metal ions and the amino acid leucine. Most bacterial species show chemotaxis, and some can sense and move toward stimuli such as light (phototaxis) and even magnetic fields (magnetotaxis).

Bacterial chemotaxis achieves remarkable performance despite the great physical limitations faced by the bacteria. Bacteria can detect concentration gradients as small as a change of one molecule per cell volume per micron and function in background concentrations spanning over five orders of magnitude. All this is done while being buffeted by Brownian noise, such that if the cell tries to swim straight for 10 sec, its orientation is randomized by 90° on average. How does *E. coli* manage to move up gradients of attractants despite these physical challenges? It is evidently too small to sense the gradient along the length of its own body.[1] The answer was discovered by Howard Berg in the early 1970s: *E. coli* uses **temporal gradients** to guide its motion. It uses a biased-random-walk strategy to sample space and convert spatial gradients to temporal

[1] Noise prohibits a detection system based on differences between two antennae at the two cell ends. To see this, note that *E. coli*, whose length is about 1 micron, can sense gradients as small as 1 molecule per micron in a background of 1000 molecules per cell volume. The Poisson fluctuations of the background signal, $\sqrt{1000} \sim 30$, mask this tiny gradient, unless integrated over prohibitively long times. Larger eukaryotic cells, whose size is on the order of 10 µm and whose responses are on the order of minutes, appear to sense spatial gradients directly.

ones. In liquid environments, *E. coli* swims in a pattern that resembles a random walk. The motion is composed of **runs**, in which the cell keeps a rather constant direction, and **tumbles**, in which the bacterium stops and randomly changes direction (Figure 7.2). The runs last about 1 sec on average and the tumbles about 0.1 sec.

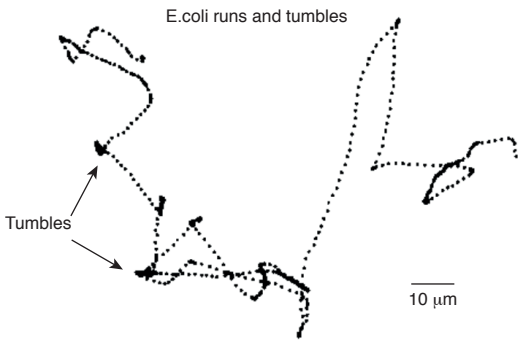

Figure 7.2

To sense gradients, *E. coli* compares the current attractant concentration to the concentration in the past. When *E. coli* moves up a gradient of attractant, it detects a net positive change in attractant concentration. As a result, it reduces the probability of a tumble (it reduces its **tumbling frequency**) and tends to continue going up the gradient. The reverse is true for repellents: if it detects that the concentration of repellent increases with time, the cell increases its tumbling frequency, and thus tends to change direction and avoid swimming toward repellents. Thus, chemotaxis senses the temporal derivative of the concentration of attractants and repellents. It follows a simple strategy: If life is getting better, keep going, and if life is getting worse, change direction.

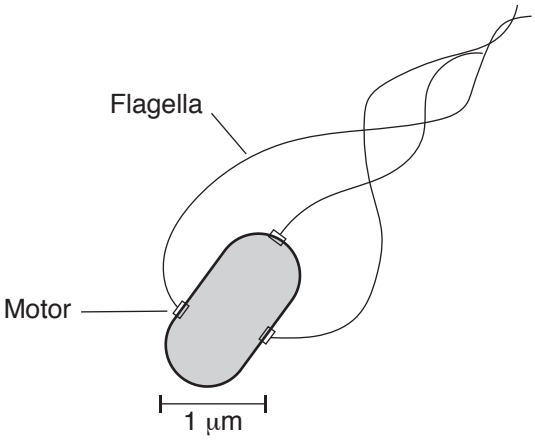

Figure 7.3

The runs and tumbles are generated by different states of the motors that rotate the bacterial flagella. Each cell has several flagella motors (Figure 7.3; see also Section 5.5XX) that can rotate either clockwise (CW) or counterclockwise (CCW). When the motors turn CCW, the flagella rotate together in a bundle and push the cell forward. When one of the motors turns CW, its flagellum breaks from the bundle and causes the cell to tumble about and randomize its orientation. When the motor turns CCW, the bundle is reformed and the cell swims in a new direction (Figure 7.4).

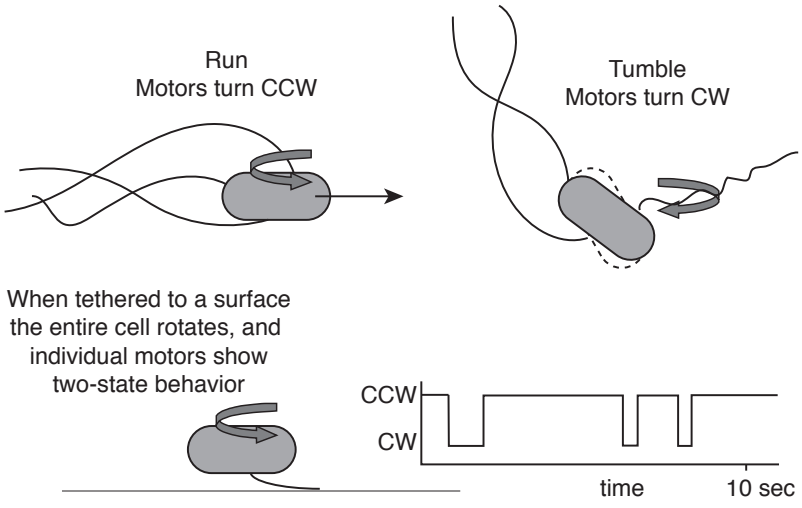

Figure 7.4

7.2.2 Response and exact adaptation

The basic features of the chemotaxis response can be described by a simple experiment. In this experiment, bacteria are observed under a microscope swimming in a liquid with no gradients. The cells display runs and tumbles, with an average **steady-state tumbling frequency** f, on the order of f ~ 1 sec^{-1}.

We now add an attractant such as aspartate to the liquid, uniformly in space. The attractant concentration thus increases at once, but no spatial gradients are formed. The cells sense an increase in attractant levels, no matter which direction they are swimming. They think that things are getting better and suppress tumbles: the tumbling frequency of the cells plummets within about 0.1 sec (Figure 7.5).

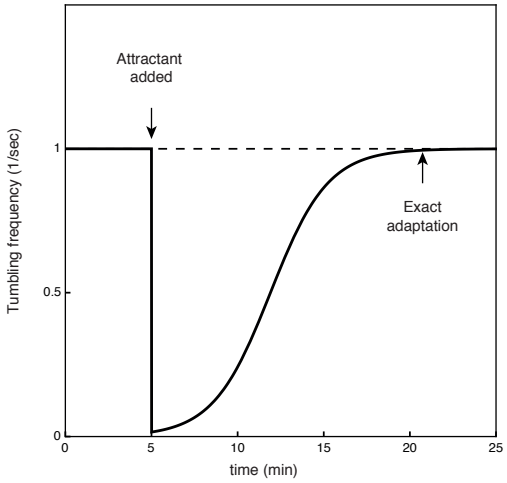

Figure 7.5

After a while, however, the cells realize they have been fooled. The tumbling frequency of the cells begins to increase, even though attractant is still present (Figure 7.5). This process, called **sensory adaptation**, is common to many biological sensory systems. For example, when we move from light to dark, our eyes at first cannot see well, but they soon adapt to sense small changes in contrast. Adaptation in bacterial chemotaxis takes several seconds to several minutes, depending on the size of the attractant step.[2]

Bacterial chemotaxis shows **exact adaptation**: the tumbling frequency in the presence of attractant returns to the same level as before attractant was added. In other words, *the steady-state tumbling frequency is independent of attractant levels*. If more attractant is now added, the cells again show a decrease in tumbling frequency, followed by exact adaptation. Changes in attractant concentration can be sensed as long as attractant levels do not saturate the receptors that detect the attractant.

Exact adaptation poises the sensory system at an activity level where it can respond to multiple steps of the same attractant, as well as to changes in the concentration of other attractants and repellents that can occur at the same time. It prevents the system from straying away from a favorable steady-state tumbling frequency that is required to efficiently scan space by random walk.

7.3 The chemotaxis protein circuit

We now look inside the *E. coli* cell and describe the protein circuit that performs the response and adaptation computations. The input to this circuit is the attractant concentration, and its output is the probability that motors turn CW, which determines the cells' tumbling frequency (Figure 7.6). The chemotaxis circuit was worked out using genetics, physiology, and biochemistry, starting with J. Adler in the late 1960s, followed by several labs, including those of D. Koshland, S. Parkinson, M.

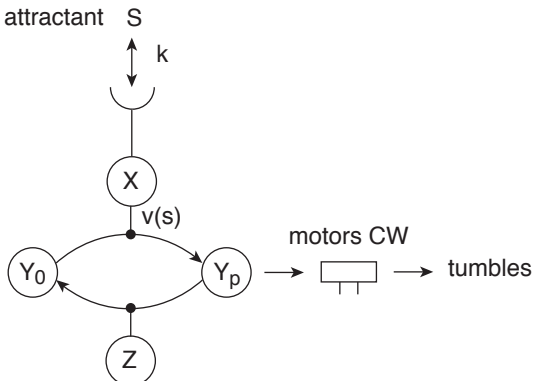

Figure 7.6

[2] Each individual cell has a fluctuating tumbling frequency signal, so that the tumbling frequency varies from cell to cell and also varies along time for any given cell (Ishihara et al., 1983; Korobkova et al., 2004). The behavior of each cell shows the response and adaptation characteristics within this noise

Simon, J. Stock, and others. The broad biochemical mechanisms of this circuit are shared with many signaling pathways in all types of cells.

Attractant and repellent molecules are sensed by specialized detector proteins called **receptors**. Each receptor protein passes through the cell's inner membrane, and has one part outside of the cell membrane and one part inside the cell. It can thus pass information from the outside to the inside of the cell. The attractant and repellent molecules bound by a receptor are called its **ligands**.

E. coli has five types of receptors, each of which can sense several ligands. There are a total of several thousand receptor proteins in each cell. They are localized in a cluster on the inner membrane, such that ligand binding to one receptor appears to affect the state of neighboring receptors. Thus, a single ligand binding event is amplified, because it can affect more than one receptor (Bray, 2002), increasing the sensitivity of this molecular detection device (Segall et al., 1986; Jasuja et al., 1999; Sourjik and Berg, 2004).

Inside the cell, each receptor is bound to a protein kinase called CheA.[3] We will consider the receptor and the kinase as a single entity, called X. X transits rapidly between two states, active (denoted X*) and inactive, on a timescale of microseconds. When X is active, X*, it causes a modification to a response-regulator protein, CheY which we will denote Y, which diffuses in the cell. This modification is the addition of a phosphoryl group (PO_4) to Y to form Yp. This type of modification, called **phosphorylation**, is used by most types of cells to pass bits of information among signaling proteins, as we saw in Chapter 6. Yp can bind the flagella motor and increase the probability that it switches from CCW to CW rotation. Thus, the higher the concentration of Yp, the higher the tumbling frequency (Cluzel et al., 2000). The phosphorylation of Yp is removed by the phosphatase CheZ, denoted Z. At steady-state, the opposing actions of X* and Z lead to a steady-state Yp level and a steady-state tumbling frequency. Thus, the main pathway in the circuit is phosphorylation of Y by X*, leading to tumbles (Fig 7.6). We now turn to the mechanism by which attractant and repellent ligands can affect the tumbling frequency.

7.3.1 Attractants lower the activity of X

When a ligand S binds receptor X, it changes the probability[4] that X will assume its active state X*. The concentration of X in its active state is called the **activity of X**. Binding of an attractant *lowers* the activity of X. Therefore, attractants reduce the rate $v(S)$ at which X phosphorylates Y, and levels of Yp drop, resulting in fewer tumbles. These responses occur within less than 0.1 sec. The response time is mainly limited by the time it takes Yp to diffuse over the length of the cells to the motors that are distributed all around the cell membrane.

---

[3] The chemotaxis genes and proteins are named with the three-letter prefix *che*, signifying that mutants in these genes are unable to perform chemotaxis.

[4] Note the strong separation of timescales. The conformation transitions between X and X* are on a microsecond timescale. Ligands remain bound to the receptor for about 1 msec. Therefore, many transitions occur within a single-ligand binding event. The activity X* is obtained by averaging over many transitions (Asakura and Honda, 1984; Mello et al., 2004; Keymer et al., 2006). Phosphorylation–dephosphorylation reactions equilibrate on the 0.1-sec timescale, and methylations occur on the sec-minute timescale.

The pathway from X to Y to the motor explains the initial response in Figure 7.5, in which attractant leads to reduction in tumbling. The reduction in activity X* due to the binding of attractant S is well described by a Hill function (Fig 7.7)

$$X^* = \frac{X_{max}}{1 + \left(\frac{S}{K}\right)^n}$$

Where Xmax is the maximal activity (this equation is ineact near S=0, see appendix XX). The halfway-point for reduction in activity is K, the binding constant of the attractant to the receptor. The Hill coefficient n is due to clusters of n receptors that show cooperativity: binding of ligand to one receptor in the cluster changes the conformation of the other receptors in the cluster and raises the affinity of ligand to the other receptors.

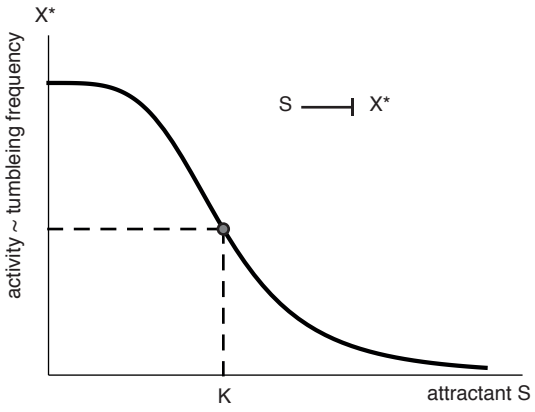

Figure 7.7

If this was all, ligand S would cause activity X^* and hence tumbling frequency to drop and stay low. What causes adaptation?

7.3.2 Adaptation is due to slow modification of X that increases its activity

The chemotaxis circuit has a second pathway devoted to adaptation. As we saw, binding of ligand reduces the activity of the receptor X. However, each receptor has several biochemical "buttons" that can be pressed to increase its activity and compensate for the effect of the attractant (Fig 7.8). These buttons are **methylation** modifications, in which a methyl group (CH_3) is added to four or five locations on the receptor. Each receptor can thus have between zero and five methyl modifications. The more methyl groups that are added, the higher the activity of the receptor.

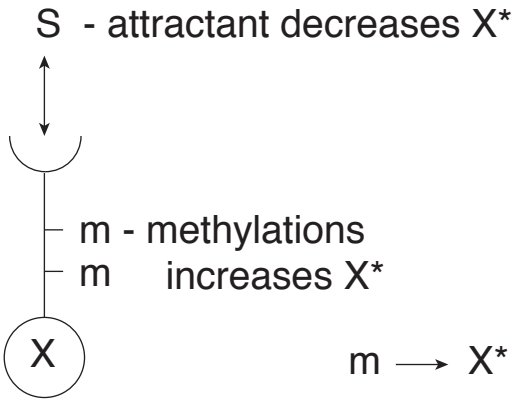

Figure 7.8

The methylation buttons work by changing the binding constant K of the receptor to attractants[5]. The more methylated the receptor the higher is K (lower chemical affinity to the attractant), (Fig 7.9). Therefore, the less attractant it binds, so that there is less inhibition of X activity, X*. In this way, methylation increases receptor activity.

Mathematically, we can describe the effect of methylation on K using the concept of free energy ΔG. The binding constant K is given by the exponential of the free energy of binding the ligand $K = e^{\Delta G}$ (the Boltzmann constant $k_b T$ is included in ΔG) . Each methylation adds some free energy γ to the bound state of the receptor, making it less favorable, so that $\Delta G = \Delta G_0 + \gamma m$, where m is the number of methylations. As a result, K increases with methylation, $\sim e^{\gamma m}$, raising the half-way-point ligand level needed for inhibition of

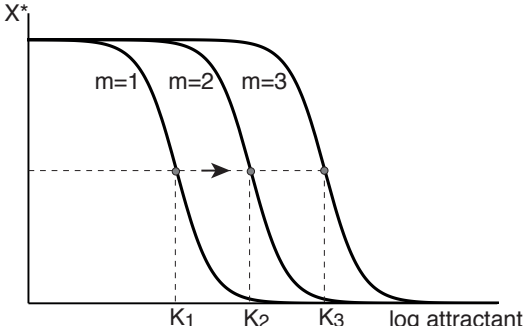

Figure 7.9

activity, Figure 7.9. The higher the methylation, the higher the half-way point for binding K, and more ligand is needed to reduce the activity X*.

Methylation of the receptors is catalyzed by a protein called CheR and is removed by an a protein called CheB, denoted R and B. Methyl groups are continually added and removed by these two antagonistic proteins, regardless of whether the bacterium senses any ligands (Fig 7.10). This seemingly wasteful cycle has an important function: it allows cells to adapt.

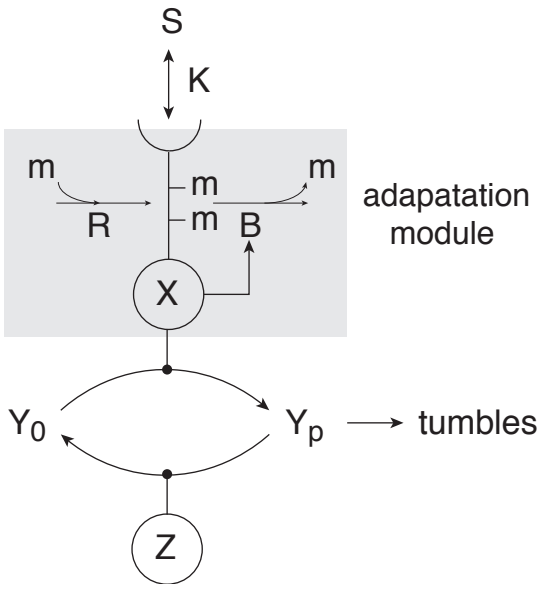

Figure 7.10

Adaptation is carried out by a negative feedback loop through B. This protein removes methyl groups only from receptors in their active conformation, X*. Thus, reduced X activity means that B is less active, causing a reduction in the rate at which methyl groups are removed by B. Methyl groups are still added, though, by R at an unchanged rate. Therefore, methylation increases. Methylation makes the receptor more active, the tumbling frequency increases. Thus, the receptors X first become less active due to attractant binding, and then methylation level gradually increases, restoring X activity. This is a negative feedback loop with a slow arm in which X* reduces methylation, and a fast arm which methylation raises X* (Fig 7.11).

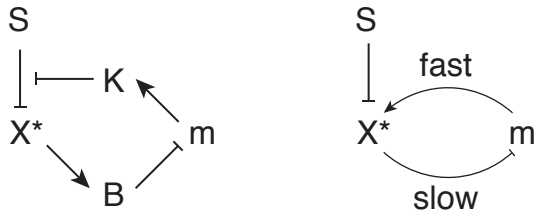

Figure 7.11

Methylation reactions are indeed much slower than the reactions in the main pathway from X to Yp to the motor (the former are on the timescale of seconds to minutes, and the latter on a sub-second timescale). The protein R is present at low amounts in the cell, about 100 copies, and appears to act at saturation (zero-order kinetics). The slow rate of the methylation reactions explains why the recovery phase of the tumbling frequency during adaptation is much slower than the initial response.

The feedback circuit is designed so that exact adaptation is achieved. That is, the increased methylation of X *precisely balances* the reduction in activity caused by the attractant. How is this precise balance achieved? Understanding exact adaptation is the goal of the model that we will next describe.

7.4 The Barkai-Leibler model of exact adaptation

Early models of chemotaxis used equations to describe the reactions just described, and showed response to attractant and exact adaptation. However, in these models, exact adaptation depended on setting specific values for parameters such as the numbers of R and B proteins per cell. These parameters had to be tuned so that methylation could exactly compensate for the reduction in activity caused by attractant. Changing the protein level parameters ruined exact adaptation (Fig 7.12). After adding attractant, the cells responded, but then returned to a different basal activity than before the

attractant step. We say that exact adaptation in these models is **fine tuned.** A fine-tuned model is described in solved exercise X.X.

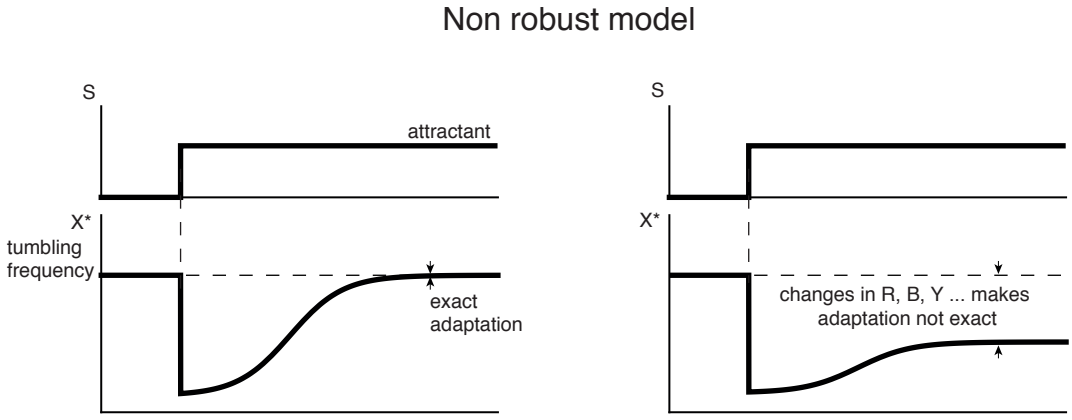

Figure 7.12

robust mechanism for exact adaptation was proposed by Naama Barkai and Stan Leibler. In this mechanism, changing parameters such as R and B protein levels changes the steady-state activity. But changing parameters does not ruin exact adaptation: after a step of attractant, activity first drops but then returns to the pre-step level (Fig 7.13).

The full model includes several methylation sites and other details, and reproduces many

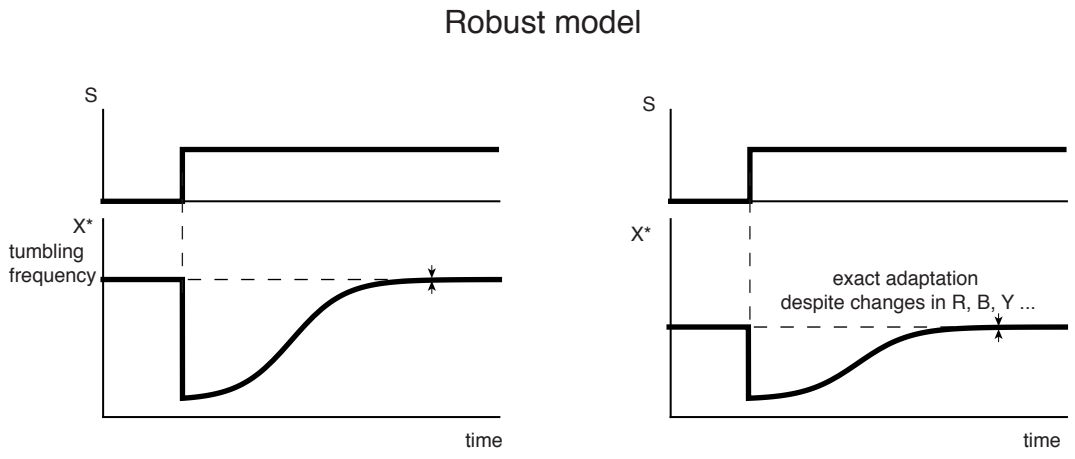

Figure 7.13

observations on the dynamical behavior of the chemotaxis system (a two-methylation-site version is solved in exercise 7.X). Here we will analyze a simplified version of the Barkai–Leibler model, aiming to understand how a biochemical circuit can robustly adapt.

The Barkai-Leibler mechanism depends on two molecular features. First, R works at a constant rate independent of its substrate, un-methylated receptors. This constant rate occurs because R is found at such low numbers and works so slowly that it always has a methylated receptor to add a methyl group to. R thus works at saturation- it adds methyl groups at a rate Vr R, where R is the number of R proteins and Vr is the rate. Second, the enzyme B works only on *active* receptors, X*. Its rate of removing methyl groups is thus Vb B X*, where B is the number of B proteins in the cell, Vb is their rate and X* is the activity.

The rate of change of the total number of methyl groups bound to the receptors, m, is given by the difference between the rates of adding methyl by R and removing them by B:

dm/dt=Vr R- Vb B X*

The steady state solution (dm/dt=0) occurs at

X*st=VrR/VbB.

Importantly, X^*_{st} *does not depend on attractant concentration*. This means that our system always returns to the same activity level regardless of input signal: we have exact adaptation.

A rate plot of this equation, Fig 7.14, shows that if X* is smaller than X*st, then methylation exceed removal, as a result X* rises, stopping when X*=X*st. Likewise, when X* exceeds X*st, removal exceeds methylation, and activity X* drops until it = goes back down to X*st. The important point is that X*st does not depend on attractant or repellant levels. Changing parameters like R and B changes X*st. But for given R and B, activity X*st always returns to its baseline level X*st. Exact adaptation is robust. Figure 7.13 shows the dynamics of this model for two sets of parameters, in which R levels are varied by a factor of 2. It is seen that the steady-state activity changes, but adaptation remains exact.

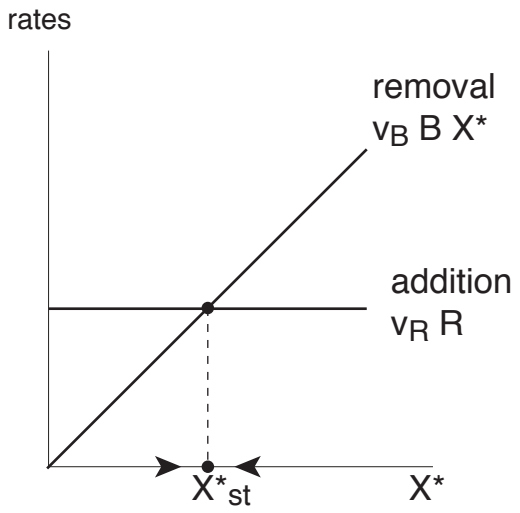

Figure 7.14

Let's review how this mechanism works. Initially the system is at steady state X*st (7.15 timepoint a). When attractant S is added, it binds the receptors and reduces their activity (Fig 7.15, tiempoint b) . Activity X* drops below X*_st within 0.1 sec. This causes the abrupt initial drop in tumbling frequency that is observed in the experiments (Figure 7.10). After this sharp initial response, adaptation occurs because B only works on the active receptors. The rate of demethylation by CheB is reduced because of the decrease in active receptors caused by the attractant. R, on the other hand, continues to methylate receptors at a constant rate. Therefore, methylation m gradually increases (Fig 7.15 timeplont c). Methylation increases the probability of receptors to be in their active state. Steady-state is reached when the number of active receptors reaches a level that balances the effects of R and B, returning to the steady-state activity level $X^* = X^*_{st}$. (Fig 7.15 timepoint d). The activity is equal to the pre-attractant activity, despite the presence of attractant. We have exact adaptation.

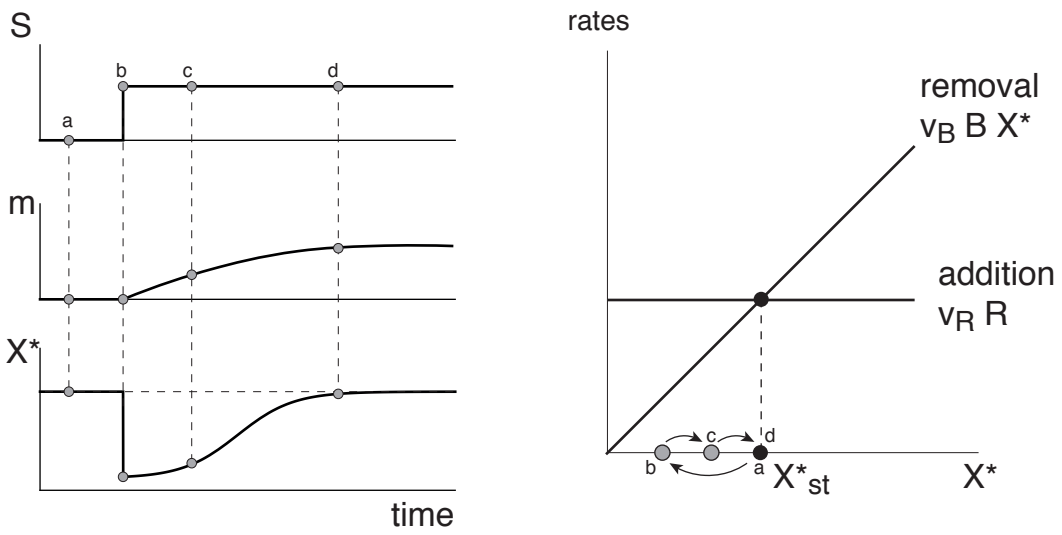

Figure 7.15

Exact adaptation occurs for a wide range of variations in any of the parameters of the model, such as V_R, V_B, R, and B. In contrast, the value of the steady-state activity to which the cells adapt depends on these parameters. In other words, steady-state activity is a *fine-tuned* feature of this model (Figure 7.10). Exact adaptation, in which the steady-state does not depend on ligand levels, is a *robust* feature of the model and does not depend on the precise values of the biochemical parameters.

There are limits to robustness. For example, if receptors become fully methylated, they can no longer compensate for attractants. Indeed, exact adaptation is broken in the case of some attractants such as serine: the serine receptor (Tsr) even when fully methylated cannot compensate for high concentrations of serine, and there no exact adaptation at high concentrations of serine.

Robustness of exact adaptation in this model depends on the assumption that B works only on active receptors, and does not demethylate receptors that are in their inactive state. This is a specific biochemical detail that is essential for robust adaptation. The assumption that CheB works only on active receptors is not unrealistic, because proteins can be exquisitely specific in discriminating between molecular states. Relaxing this assumption by allowing a small relative rate ε for B action on inactive receptors entails a loss of exact adaptation by a factor on the order of ε.

Robust adaptation and Integral feedback

At the heart of this mechanism is a feedback loop called **integral feedback** (Yi et al 2000), which is a central principle in engineering. In integral feedback, there is a slow component (methylation in our case) which integrates an 'error' over time, and acts to decrease the error. In chemotaxis, the error is the distance between the activity and the steady-state activity $error = X^*_{st} - X^*$. The power of integral feedback is that as long as the error is not zero, the integrator keeps accumulating, and the feedback grows until it forces the error to go to zero. There is no choice for the system but to return to X^*_{st}.

The mapping of the Barkai-Leibler model and integral feedback is easiest to by rewriting the equation for the dynamcis of methylation:

$$\frac{dm}{dt} = VbB(X^*_{st} - X^*)$$

Solving this equation by taking an integral over time on both sides shows that methylation integrates over the error :

$m(t) \sim \int_{-\infty}^{t} (X_{st}^* - X^*(t))\, dt \sim \int error(t) dt$

Because of this integrator effect, the feedback does not stop until the error is zero (until $X^* = X_{st}^*$). Even a small error keeps being integrated over time to lead to a large feedback signal. Linearity is not crucial here: It is enough that dm/dt=g(X*) , with g(X*) a decreasing function of a that crosses zero at X*_st, f(X*_st)=0, to show integral feedback and exact adaptation.

Engineers use integral feedback to achieve exact adaptation in many familiar situations. For example, integral feedback ensures that a heater can keep the temperature T of a room at a desired set-point T_st. This integral feedback controller, in which the power to the heater is governed by the integrated error (T-Tst), is shown in solved exercise XX. The heater power changes slowly and is analogous to methylation.

To summarize, we put together the equations for ligand binding and methylation, to arrive at a model for bacterial chemotaxis that captures many experiments on the dynamic response to changing ligands. We will use this model, which is a simplified version of a model presented by Tu Shimizu and Berg, in the next chapter. The model becomes simpler when we use the receptor binding constant K as a variable instead of m. To do so, we use the relation $K \sim e^{\gamma m}$ and hence $\frac{dK}{dt} \sim K dm/dt$. We also use as the output the receptor activity normalized by its maximal value a=X*/X_max:

$(1) dK/dt = cK(a_{st} - a)$

$(2) a = 1/(1 + (S/K)^n)$

Parameters that match experimental data are ast=0.3, c=1 min^-1 and n=6. Fig 7.XX shows how the activity a drops after step additions of attractant, and shows a pronounced pulse when attractant is removed. Exact adaptation occurs in all cases, as the binding constant K slowly adjusts to the changes in input. K acts like an internal representation of the external signal S.

When attractant S is added, activity a(t) drops thanks to equation 2. As a result the receptor halfway-point K(t) rises slowly thanks to equation 1. Its as if the receptor adjusts its half-way point K to be sensitive near the new level of attractant. This is like gain-control in a camera, which adjusts its sensitivity to the ambient level of light. Thanks to the integral feedback equation, the adjusting process of K stops precisely when activity reaches its set point a_st. Without exact adaptation, the receptors could not be sensitive over many orders of magnitude of attractant levels, any more than a camera without gain control could work across orders of magnitude of light.

7.4.4 Experiments show that exact adaptation is robust, whereas steady-state activity and adaptation times are fine tuned

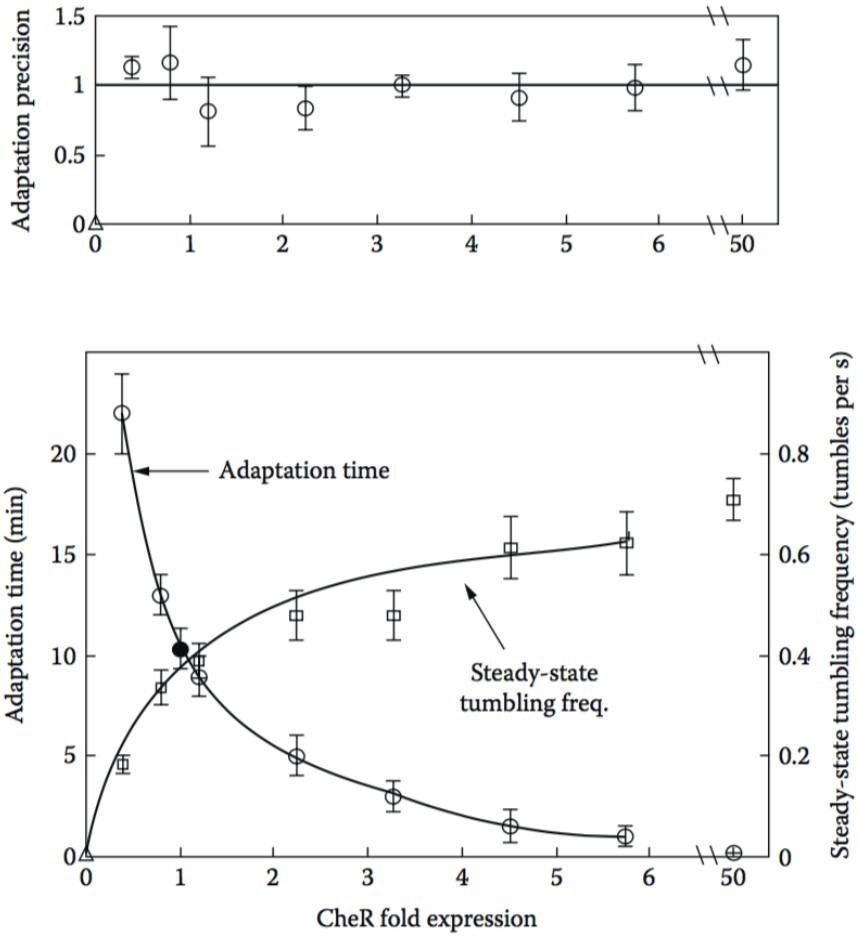

Figure 7.16

An experimental test of robustness employed genetically engineered *E. coli* strains, which allowed controlled changes in the concentration of each of the chemotaxis proteins (Alon et al., 1999). This control was achieved by first deleting the gene for one chemotaxis protein (for example, R) from the chromosome, and then introducing into the cell a copy of the gene under control of an inducible promoter (the *lac* promoter). Thus, expression of the protein was controlled by means of an externally added chemical inducer (IPTG). The more inducer added, the higher the R concentration in the cells. In this way, R levels were varied from about 0.5 to 50 times their wild-type levels. The population response of these cells to a saturating step of attractant was monitored using video microscopy on swimming cells. The experiment was carried out with changes in the expression levels of different chemotaxis proteins.

It was found that the steady-state tumbling frequency and the adaptation time varied with the levels of the proteins that make up the chemotaxis network (Figure 7.16). For example, steady-state tumbling frequency increased with increasing CheR levels, whereas adaptation time decreased. Despite these variations, exact adaptation remained robust to within experimental error. These results support the robust model for exact adaptation.

This experiment, which took three years, was the way that I transitioned from theoretical physics to experimental biology in my postdoc with Stanislas Leibler at Princeton. I got a lot of help from Mike Surrette who was a postdoc working on bacterial chemotaxis in the Stock lab next door. My fascination with the robust model was powerful enough to help me make the transformation from theorist to experimentalist.

7.5 Individuality and robustness in bacterial chemotaxis

Spudich and Koshland (1976) observed that genetically identical bacterial cells appear to have an individual character as they perform chemotaxis. Some cells are "nervous" and tumble more frequently than others, whereas other cells are "relaxed" and swim with fewer tumbles than the norm. These individual characteristics of each cell last for tens of minutes. The adaptation time to an attractant stimulus also varies from cell to cell. Interestingly, these two features are correlated: the

steady-state tumbling frequency f in a given cell is inversely correlated with its adaptation time, τ, that is, $f \sim 1/\tau$.

The robust model for bacterial chemotaxis can supply an explanation for the varying chemotaxis personalities of *E. coli* cells. This is based on the cell–cell variation in chemotaxis protein levels, and particularly in the least abundant protein in the system, tions in R affect the tumbling frequency f and the adaptation time τ in opposite directions. The Barkai–Leibler model with multiple methylation sites suggests that $f \sim R$ and $\tau \sim 1/R$. Thus, the model predicts that $f \sim 1/\tau$, explaining the observed correlation in these two features (see solved exercise 7.X). [6]

Despite the cell–cell variability in tumbling frequency, the vast majority of the cells in a population perform chemotaxis and climb gradients of attractants. On the other hand, mutant cells that have wild-type tumbling frequency but cannot adapt precisely (such as certain mutants in both CheR and CheB) are severely defective in chemotaxis ability. Evidently, tumbling frequency need not be precisely tuned for successful chemotaxis, whereas exact adaptation is important for most ligands.[1]

In fact, there is an advantage in having a range of tumbling frequencies in a population of bacteria. This is because bacteria cannot know in advance which type of medium they will be moving through. In a free liquid, it is optimal to have long runs to sample space widely (Fig 7.17). But in a liquid dense with obstacles, as occurs in the crowded environments of the soil or the lower intestine, it is optimal to have shorter runs to avoid being stuck against an obstacle for long times. Thus, variation in protein levels can generate a **bet hedging** strategy in which different individuals are suited for different possible future environment. Not all of the eggs are in one basket. Thanks to robustness, no matter what the steady-state tumbling frequency is, every individual will have exact adaptation, and hence be able to work across many orders of magnitude of signal.

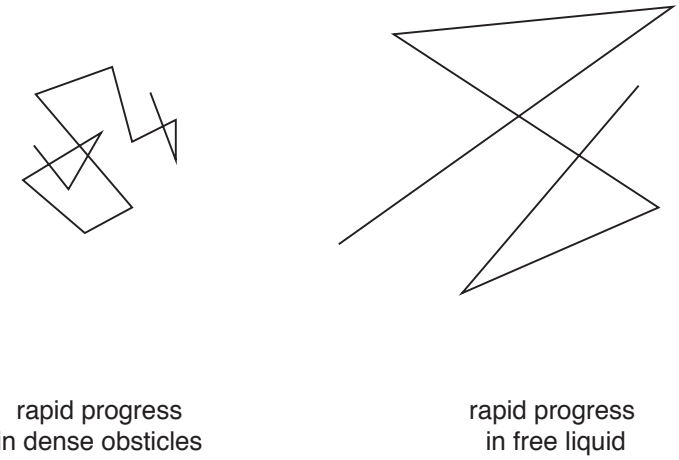

Figure 7.17

In summary, the bacterial chemotaxis circuit has a design such that a key feature (exact adaptation) is robust with respect to variations in protein levels. Other features, such as steady-state activity and adaptation times, are fine-tuned. These latter features show variations within a population due to intrinsic cell–cell variations in protein levels. Because of the robust design, the intrinsic variability in the cell's protein levels does not abolish exact adaptation.

As a theorist, one can usually write many different models to describe a given biological system, especially if some of the biochemical interactions are not fully characterized. Of these models, only very few will typically be robust with respect to variations in the components. Thus, the robustness principle can help narrow down the range of models that work on paper to the few that can work in the cell. Robust design is an important factor in determining the specific types of

[6] Detailed stochastic simulations of this protein circuit were pioneered by D. Bray and colleagues (Shimizu et al., 2003).

circuits that appear in cells. In the next chapter, we will study how robustness constraints can shape the circuits that guide pattern formation in embryonic development.

Further reading

Alon, U., Surette, M.G., Barkai, N., and Leibler, S. (1999). Robustness in bacterial chemotaxis. *Nature*, 397: 168–171.

Barkai, N. and Leibler, S. (1997). Robustness in simple biochemical networks. *Nature*, 387: 913–917.

Berg, H.C. (2003). *E. coli in Motion*. Springer.

Berg, H.C. and Brown, D.A. (1972). Chemotaxis in *Escherichia coli* analyzed by three-dimensional tracking. *Nature,* 239: 500–504.

Berg, H.C. and Purcell, E.M. (1977). Physics of chemoreception. *Biophys. J.,* 20: 193–219.

Knox, B.E., Devreotes, P.N., Goldbeter, A., and Segel, L.A. (1986). A molecular mechanism for sensory adaptation based on ligand-induced receptor modification. *Proc. Natl. Acad. Sci. U.S.A.*, 83: 2345–2349.

Kollmann, M., Lovdok, L., Bartholome, K., Timmer, J., and Sourjik, V., (2005). Design principles of a bacterial signalling network. *Nature*, 438: 504–507.

Spudich, J.L. and Koshland, D.E., Jr. (1976). Non-genetic individuality: chance in the single cell. *Nature*, 262: 467–471.

Yi, T.M., Huang, Y., Simon, M.I., and Doyle, J. (2000). Robust perfect adaptation in bacterial chemotaxis through integral feedback control. *Proc. Natl. Acad. Sci. U.S.A.,* 97: 4649–4653.